



Relaxation Dynamics in Atomic-Molecular Bose Condensates in the Presence of Gaussian Noise

Avinaba Mukherjee ^{1,*} and Raka Dasgupta ^{1,†}

¹*Department of Physics, University of Calcutta, 92 A. P. C. Road, Kolkata 700009, India*

(Dated: July 25, 2025)

We investigate the dynamics of atomic and molecular bosons weakly coupled via Feshbach detuning in the presence of Gaussian white noise. The time-evolution of the population imbalance between the two species, as well as the coherence of the system are analyzed using a Bloch sphere model. We observe that the system exhibits relaxation of the Bloch vector components towards a stable equilibrium. In the population imbalance dynamics, the relaxation rates predicted by the Bogoliubov Born Green Kirkwood Yvon (BBGKY) hierarchy are found to be smaller than those calculated with a simple the mean field approximation. As for the coherence dynamics, the inclusion of correlations and fluctuations in the system can either increase or decrease the relaxation time, depending on the initial conditions. We attribute the increase in the relaxation time to the emergence of a structured noise, and the subsequent suppression of certain dephasing channels. We also study the impact of correlations and fluctuations on time-averaged quantities like the drift speed, the fringe visibility, the phase entanglement etc., and find the results to be in perfect agreement with the properties of the relaxation dynamics.

I. INTRODUCTION

A system of coupled atomic-molecular Bose-Einstein condensates (BECs) acts as an interesting platform that has inspired a wide range of scientific investigations in recent times[1–16]. Here, two atomic bosons can form a molecular boson via Feshbach resonance [17, 18]. This system effectively functions as a Bosonic Josephson Junction. Although conventional josephson junctions are created by trapping a BEC in a double well potential, [19–38], a coupled atomic-molecular BEC system serves a somewhat similar purpose because it, too, consists of two weakly coupled macroscopic quantum states. The Feshbach coupling between the atomic and molecular bosons here plays the role of tunneling. In addition, the atomic-BEC (A-BEC) and molecular-BEC (M-BEC) states are separated by a threshold energy of molecule formation: analogous to the intermediate insulating layer in superconducting Josephson junctions.

The non-equilibrium dynamics of bosonic josephson junctions [39–44] is an emerging area of research. Two-mode BEC in a double well manifests a damped oscillation of population imbalance and relative phase towards a stable equilibrium point if the hopping amplitude and detuning are corrupted by Gaussian white Noise [45]. If one considers quantum fluctuations described by the Bogoliubov Back-reaction (BBR) formalism beyond the Mean-Field (MF) or classical regime in such a two-mode condensate, it is observed that decoherence in the system either enhances or suppresses phase diffusion [46]. For an atomic-molecular BEC system, it was observed that the conversion dynamics in the presence of phase noise is well-described using MF for a short time scale, but for a longer time scale, the BBR correction is necessary [47].

In this work, we theoretically study the relaxation dynamics of a Feshbach-coupled atomic-molecular BECs system, with a focus on the particle-imbalance between two quantum states, as well as the coherence. The system can be fully described in

terms of the components of the Bloch vector: \hat{L}_x , \hat{L}_y and \hat{L}_z . We find that when Gaussian White Noise corrupts the coupling strength and detuning, both MF and BBR treatment of the Hamiltonian lead to damped oscillatory dynamics for the Bloch vector components. However, the estimated relaxation time differs substantially from MF to BBR, i.e. it depends on higher-order correlation (self- or mutual) between the components. The longitudinal relaxation time T_z and the transverse relaxation rate T_{x-y} of the three components of the Bloch vector are substantially affected by the variance and covariance of \hat{L}_x , \hat{L}_y and \hat{L}_z . We try to relate our results to several related physical parameters: (i) drift speed, (ii) fringe visibility, (iii) phase entanglement, and (iv) polar or precession angle of Bloch sphere.

The divisions of the paper are as follows. In Sec. II, We establish the basic model, and derive the dynamical equations to include the effect of noise on the system. Then in Sec. III, we study the relaxation dynamics using both MF and BBR frameworks. In Sec. IV, we calculate the time-averaged values of quantities like fringe visibility, and phase entanglement, and connect these findings with the trends in the relaxation processes. In Sec. V, we summarize our results.

II. BASIC MODEL

We consider an ultracold system in which two bosonic atoms combine to form a bosonic molecule through a Feshbach resonance process[48–50]. We treat the system in a two-channel model, consisting of a closed channel and an open or entrance channel [51]. When the energy of the entrance channel matches that of the closed channel, the bosonic atoms are resonantly coupled to form bosonic dimers. The energy difference between the A-BEC and M-BEC states is the Feshbach detuning ϵ_b , and this can be tuned using an external magnetic field. The system is described by the following Hamiltonian [52–55].

$$\hat{H} = \frac{u_1}{2} \hat{a}^\dagger \hat{a}^\dagger \hat{a} \hat{a} + \frac{u_2}{2} \hat{b}^\dagger \hat{b}^\dagger \hat{b} \hat{b} + u_3 \hat{a}^\dagger \hat{b}^\dagger \hat{b} \hat{a} + g(\hat{a}^\dagger \hat{a}^\dagger \hat{b} + \hat{b}^\dagger \hat{a} \hat{a}) + \epsilon_b \hat{b}^\dagger \hat{b} \quad (1)$$

Here, \hat{a}^\dagger and \hat{a} are the atomic creation and annihilation operators, while \hat{b}^\dagger and \hat{b} are their molecular counterparts. Here, u_1 and u_2 represent atom-atom interaction and molecule-molecule interaction strength; u_3 is an interaction between bosonic atoms and bosonic molecules, and g is the Feshbach coupling constant.

In Sec. II A, we recast the system Hamiltonian in terms of Bloch vector's components and then study the coherent evolution of each component. Next, Gaussian white noises are applied on both the Feshbach coupling strength and detuning, and the incoherent evolution of the Bloch vector components are analyzed using the Ito calculus in Sec. II B.

A. Bloch vector description of the two-mode condensate

The Bloch vector's components or Schwinger pseudo-spin operators [56, 57] are introduced as follows [47, 58]

$$\hat{L}_x = \frac{\sqrt{2}}{N^{\frac{3}{2}}} (\hat{a}^\dagger \hat{a}^\dagger \hat{b} + \hat{b}^\dagger \hat{a} \hat{a}) \quad (2a)$$

$$\hat{L}_y = \frac{\sqrt{2}i}{N^{\frac{3}{2}}} (\hat{a}^\dagger \hat{a}^\dagger \hat{b} - \hat{b}^\dagger \hat{a} \hat{a}) \quad (2b)$$

$$\hat{L}_z = \frac{2\hat{b}^\dagger \hat{b} - \hat{a}^\dagger \hat{a}}{N} \quad (2c)$$

$$N = 2\hat{b}^\dagger \hat{b} + \hat{a}^\dagger \hat{a} \quad (2d)$$

\hat{L}_x and \hat{L}_y represent the real and imaginary parts of coherence, while \hat{L}_z denotes the population imbalance between atoms and molecules [59]. N is the total number of atoms in the system.

In a semi-classical approximation, the operators \hat{a} and \hat{b} in Eq. (1) can be expressed as $\hat{a} = \sqrt{N_a} e^{i\theta_a}$, and $\hat{b} = \sqrt{N_b} e^{i\theta_b}$ [52, 54, 60, 61]. Here, N_a represents the atomic population, and N_b represents the molecular population where θ_a , and θ_b are the phases of atomic and molecular condensate.

$$\hat{L}_x = \frac{(1 - \tilde{z})\sqrt{1 + \tilde{z}}}{\sqrt{2}} \cos \tilde{\phi} \quad (3a)$$

$$\hat{L}_y = \frac{(1 - \tilde{z})\sqrt{1 + \tilde{z}}}{\sqrt{2}} \sin \tilde{\phi} \quad (3b)$$

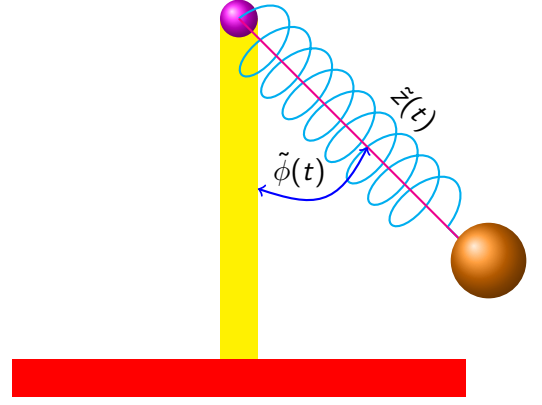


FIG. 1: The usual non-rigid pendulum model, where the point of suspension (●) is attached to the vertical stand. Since the pendulum is non-rigid, both the length $\tilde{z}(t)$ of the spring and the angle $\tilde{\phi}(t)$ of the bob (●) are time-dependent variables.

$$\hat{L}_z = \tilde{z} \quad (3c)$$

Here, $z = 2\hat{b}^\dagger \hat{b} - \hat{a}^\dagger \hat{a} = 2N_b - N_a$ represents the difference between the number of atoms between the molecular state and the atomic state; and $\tilde{\phi} = 2\theta_a - \theta_b$ is the relative phase between the atomic-molecular BEC. Eq. (3) can be mapped to a non-rigid pendulum model as shown in Fig. (1). Here, \tilde{z} and $\tilde{\phi}$ are canonically conjugate variables [59]. We would like to point out that a Bloch vector model is often used to study the population dynamics of the BEC in a double well. For an atomic-molecular condensate, the Bloch vectors can be defined just in an analogous way. However, unlike the Bloch vectors for a single condensate system in a double well [10, 46, 62], the components of the Bloch vector for the atomic-molecular condensate do not obey the usual SU(2) algebra [63–65]. Still, they are very effective for the ease of visualization of the system dynamics. The fully molecular ($|A = 0, M = 1\rangle$) and fully atomic states ($|A = 1, M = 0\rangle$) can be depicted as the North and South poles [66, 67] of the Bloch Sphere in Fig. (2).

The commutation relations of the Bloch vector components are given below [47, 68]

$$[\hat{L}_x, \hat{L}_y] = \frac{i}{N} (1 - \hat{L}_z)(1 + 3\hat{L}_z) + O(\frac{1}{N^2}) \quad (4a)$$

$$[\hat{L}_y, \hat{L}_z] = \frac{4i\hat{L}_x}{N} \quad (4b)$$

$$[\hat{L}_z, \hat{L}_x] = \frac{4i\hat{L}_y}{N} \quad (4c)$$

Moreover, $[N, \hat{L}_i] = 0$ for $i = x, y, z$.

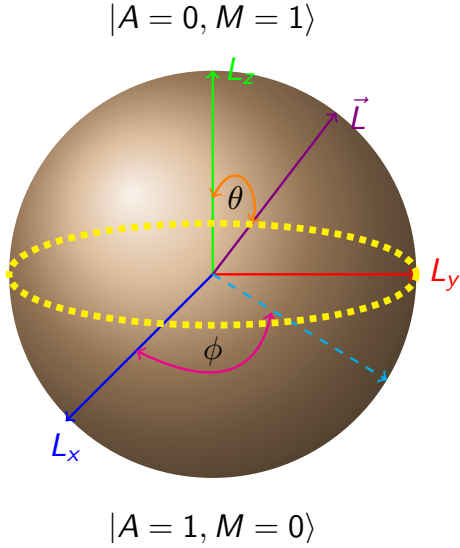


FIG. 2: The Bloch sphere model, where the North and South poles represent fully molecular (M) and atomic (A) Bose-Einstein condensates (BEC), respectively. The yellow circle denotes the equatorial plane.

Now, Eq. (1) recast in terms of Bloch vector's components becomes

$$\begin{aligned} \hat{H} = & \frac{u_1 N^2}{8} (\hat{L}_z - 1)^2 + \frac{u_1 N}{4} (\hat{L}_z - 1) + \frac{u_2 N^2}{32} (\hat{L}_z + 1)^2 \\ & - \frac{u_2 N}{8} (\hat{L}_z + 1) - \frac{u_3 N^2}{8} (\hat{L}_z^2 - 1) + \frac{g N^{\frac{3}{2}}}{\sqrt{2}} \hat{L}_x + \frac{N \epsilon_b}{4} (\hat{L}_z + 1) \end{aligned} \quad (5)$$

Rewriting $Nu_1 = U_1$, $Nu_2 = U_2$, $Nu_3 = U_3$, and $g\sqrt{N} = \tilde{g}$. Eq. (5) can be expressed as

$$\begin{aligned} \hat{H} = & \frac{U_1 N}{8} (\hat{L}_z - 1)^2 + \frac{U_1}{4} (\hat{L}_z - 1) + \frac{U_2 N}{32} (\hat{L}_z + 1)^2 \\ & - \frac{U_2}{8} (\hat{L}_z + 1) - \frac{U_3 N}{8} (\hat{L}_z^2 - 1) + \frac{\tilde{g} N}{\sqrt{2}} \hat{L}_x + \frac{N \epsilon_b}{4} (\hat{L}_z + 1) \end{aligned} \quad (6)$$

In usual experiments, [69, 70] the number of particles can be taken as 10^6 - 10^7 . Now, in large N limit, Eq. (6) becomes,

$$\begin{aligned} \hat{\mathcal{H}} = & \frac{\hat{H}}{N} = \frac{U_1}{8} (\hat{L}_z - 1)^2 + \frac{U_2}{32} (\hat{L}_z + 1)^2 \\ & - \frac{U_3}{8} (\hat{L}_z^2 - 1) + \frac{\tilde{g}}{\sqrt{2}} \hat{L}_x + \frac{\epsilon_b}{4} (\hat{L}_z + 1) \end{aligned} \quad (7)$$

The dynamical evolution of the Bloch vector's components, following Heisenberg's equation of motion, is given by :

$$\begin{aligned} \dot{\hat{L}}_x = & \left(\frac{U_3}{2\hbar} - \frac{U_2}{8\hbar} - \frac{U_1}{2\hbar} \right) (\hat{L}_y \hat{L}_z + \hat{L}_z \hat{L}_y) \\ & + \left(\frac{U_1}{\hbar} - \frac{U_2}{4\hbar} - \frac{\epsilon_b}{\hbar} \right) \hat{L}_y \end{aligned} \quad (8a)$$

$$\begin{aligned} \dot{\hat{L}}_y = & \left(\frac{U_1}{2\hbar} + \frac{U_2}{8\hbar} - \frac{U_3}{2\hbar} \right) (\hat{L}_x \hat{L}_z + \hat{L}_z \hat{L}_x) \\ & + \left(\frac{U_2}{4\hbar} - \frac{U_1}{\hbar} + \frac{\epsilon_b}{\hbar} \right) \hat{L}_x \\ & - \frac{\tilde{g}}{\sqrt{2}\hbar} \{ (1 - \hat{L}_z)(1 + 3\hat{L}_z) \} \end{aligned} \quad (8b)$$

$$\dot{\hat{L}}_z = \frac{2\sqrt{2}\tilde{g}}{\hbar} \hat{L}_y \quad (8c)$$

It is also found that $\dot{N} = 0$, i.e., the total number of atoms remain conserved.

In the following subsection (Sec. II B), we investigate the effect of applying Gaussian white noise to the parameters \tilde{g} and ϵ_b . This noise drives the system out of equilibrium, and we analyze how the system relaxes back towards its equilibrium configuration.

B. Inclusion of Noise in the dynamical equations

Next, we consider that the modified coupling (\tilde{g}) and the detuning (ϵ_b) are corrupted by white noise $n_x(t)$ and $n_z(t)$, respectively. These noises are delta-correlated Gaussian noises and their properties are as follows [71]

$$\langle n_x(t) \rangle = 0 \quad (9a)$$

$$\langle n_z(t) \rangle = 0 \quad (9b)$$

$$\langle n_x(t_1) n_x(t_2) \rangle = \Gamma_x \delta(t_1 - t_2) \quad (9c)$$

$$\langle n_z(t_1) n_z(t_2) \rangle = \Gamma_z \delta(t_1 - t_2) \quad (9d)$$

Here Γ_x and Γ_z are the strength of the noises applied to \tilde{g} and ϵ_b respectively[72]. The physical origin of Γ_x is the decoherence or dephasing due to elastic collisions between the thermal cloud and condensed particles [73–75]. On the other hand, the physical origin of Γ_z is the fluctuation of the applied magnetic field around the Feshbach resonance point [63] or the thermal fluctuation of the BEC at finite temperatures [76].

Accordingly, the dynamical relations of the Bloch vector's components are expressed as follows:

$$\begin{aligned} \dot{\hat{L}}_x = & \left(\frac{U_3}{2\hbar} - \frac{U_2}{8\hbar} - \frac{U_1}{2\hbar} \right) (\hat{L}_y \hat{L}_z + \hat{L}_z \hat{L}_y) \\ & + \left(\frac{U_1}{\hbar} - \frac{U_2}{4\hbar} - \frac{\epsilon_b + n_z(t)}{\hbar} \right) \hat{L}_y \end{aligned} \quad (10a)$$

$$\begin{aligned} \dot{\hat{L}}_y = & \left(\frac{U_1}{2\hbar} + \frac{U_2}{8\hbar} - \frac{U_3}{2\hbar} \right) (\hat{L}_x \hat{L}_z + \hat{L}_z \hat{L}_x) \\ & + \left(\frac{U_2}{4\hbar} - \frac{U_1}{\hbar} + \frac{\epsilon_b + n_z(t)}{\hbar} \right) \hat{L}_x \\ & - \frac{\tilde{g} + n_x(t)}{\sqrt{2}\hbar} (1 - \hat{L}_z)(1 + 3\hat{L}_z) \end{aligned} \quad (10b)$$

$$\dot{\hat{L}}_z = \frac{2\sqrt{2}(\tilde{g} + n_x(t))}{\hbar} \hat{L}_y \quad (10c)$$

Here $n_x = dw_x/dt$ and $n_z = dw_z/dt$ [71, 77] where w_x and w_z are Wiener processes.

$$d\hat{L}_x = \left[\left(\frac{U_3}{2\hbar} - \frac{U_2}{8\hbar} - \frac{U_1}{2\hbar} \right) (\hat{L}_y \hat{L}_z + \hat{L}_z \hat{L}_y) + \left(\frac{U_1}{\hbar} - \frac{U_2}{4\hbar} - \frac{\epsilon_b}{\hbar} \right) \hat{L}_y \right] dt - \frac{\hat{L}_y}{\hbar} dw_z \quad (11a)$$

$$d\hat{L}_y = \left[\left(\frac{U_1}{2\hbar} + \frac{U_2}{8\hbar} - \frac{U_3}{2\hbar} \right) (\hat{L}_x \hat{L}_z + \hat{L}_z \hat{L}_x) + \left(\frac{U_2}{4\hbar} - \frac{U_1}{\hbar} + \frac{\epsilon_b}{\hbar} \right) \hat{L}_x - \frac{\tilde{g}}{\sqrt{2}\hbar} (1 - \hat{L}_z)(1 + 3\hat{L}_z) \right] dt + \frac{\hat{L}_x}{\hbar} dw_z - \frac{(1 - \hat{L}_z)(1 + 3\hat{L}_z)}{\sqrt{2}\hbar} dw_x \quad (11b)$$

$$d\hat{L}_z = \frac{2\sqrt{2}\tilde{g}}{\hbar} \hat{L}_y dt + \frac{2\sqrt{2}\hat{L}_y}{\hbar} dw_x \quad (11c)$$

We have used Ito calculus on dL_j [77]. Note that $\langle dw_x \rangle = \langle dw_z \rangle = 0$, $dw_x dw_x = \gamma_x dt$ and $dw_z dw_z = \gamma_z dt$ [71, 77, 78] where γ_x and γ_z are the strengths of Wiener processes.

$$d\hat{L}_x = \left[\left(\frac{U_3}{2\hbar} - \frac{U_2}{8\hbar} - \frac{U_1}{2\hbar} \right) (\hat{L}_y \hat{L}_z + \hat{L}_z \hat{L}_y) + \left(\frac{U_1}{\hbar} - \frac{U_2}{4\hbar} - \frac{\epsilon_b}{\hbar} \right) \hat{L}_y - \frac{\gamma_z \hat{L}_x}{2\hbar^2} \right] dt - \frac{\hat{L}_y}{\hbar} dw_z \quad (12a)$$

$$d\hat{L}_y = \left[\left(\frac{U_1}{2\hbar} + \frac{U_2}{8\hbar} - \frac{U_3}{2\hbar} \right) (\hat{L}_x \hat{L}_z + \hat{L}_z \hat{L}_x) + \left(\frac{U_2}{4\hbar} - \frac{U_1}{\hbar} + \frac{\epsilon_b}{\hbar} \right) \hat{L}_x - \frac{\tilde{g}}{\sqrt{2}\hbar} (1 - \hat{L}_z)(1 + 3\hat{L}_z) + \frac{1}{2} \left\{ -\frac{4}{\hbar^2} \hat{L}_y + \frac{6}{\hbar^2} (\hat{L}_y \hat{L}_z - \hat{L}_z \hat{L}_y) \right\} \gamma_x - \frac{\hat{L}_y \gamma_z}{2\hbar^2} \right] dt - \frac{(1 - \hat{L}_z)(1 + 3\hat{L}_z)}{\sqrt{2}\hbar} dw_x + \frac{\hat{L}_x}{\hbar} dw_z \quad (12b)$$

$$d\hat{L}_z = \left(\frac{2\sqrt{2}\tilde{g}\hat{L}_y}{\hbar} - \frac{\gamma_x(1 - \hat{L}_z)(1 + 3\hat{L}_z)}{\hbar^2} \right) dt + \frac{2\sqrt{2}\hat{L}_y}{\hbar} dw_x \quad (12c)$$

If an average is taken over the noises, and the operators are replaced by their expectation values, then one obtains

$$\frac{d\langle \hat{L}_x \rangle}{dt} = \left(\frac{U_3}{2\hbar} - \frac{U_2}{8\hbar} - \frac{U_1}{2\hbar} \right) \langle \hat{L}_y \hat{L}_z + \hat{L}_z \hat{L}_y \rangle + \left(\frac{U_1}{\hbar} - \frac{U_2}{4\hbar} - \frac{\epsilon_b}{\hbar} \right) \langle \hat{L}_y \rangle - \frac{\gamma_z \langle \hat{L}_x \rangle}{2\hbar^2} \quad (13a)$$

$$\begin{aligned} \frac{d\langle \hat{L}_y \rangle}{dt} &= \left(\frac{U_1}{2\hbar} + \frac{U_2}{8\hbar} - \frac{U_3}{2\hbar} \right) \langle \hat{L}_x \hat{L}_z + \hat{L}_z \hat{L}_x \rangle \\ &+ \left(\frac{U_2}{4\hbar} - \frac{U_1}{\hbar} + \frac{\epsilon_b}{\hbar} \right) \langle \hat{L}_x \rangle - \frac{\tilde{g}}{\sqrt{2}\hbar} \langle (1 + 2\hat{L}_z - 3\hat{L}_z^2) \rangle \\ &+ \frac{\gamma_x}{\hbar^2} \langle (3\hat{L}_y \hat{L}_z + 3\hat{L}_z \hat{L}_y - 2\hat{L}_y) \rangle - \frac{\gamma_z \langle \hat{L}_y \rangle}{2\hbar^2} \end{aligned} \quad (13b)$$

$$\frac{d\langle \hat{L}_z \rangle}{dt} = \frac{2\sqrt{2}\tilde{g}\langle \hat{L}_y \rangle}{\hbar} - \frac{\gamma_x \langle (1 + 2\hat{L}_z - 3\hat{L}_z^2) \rangle}{\hbar^2} \quad (13c)$$

In the next section (Sec. III), We examine the relaxation dynamics of the Bloch vector components in both the thermodynamic (MF) and quantum (BBGKY) limits.

III. RELAXATION DYNAMICS

We study the relaxation dynamics of the Bloch vector components. First, we formulate the dynamical equations by considering only the first moment of the Bloch vector components using the mean-field (MF) approximation. Next, we extend that calculation using the Bogoliubov-Born-Green-Kirkwood-Yvon (BBGKY) framework, considering nonzero variance and covariance of these components. We solve these equations numerically for both the MF (Sec. III A) and the BBGKY calculations (Sec. III B).

A. MF

In the mean-field framework, the system is described using the expectation values of the Bloch vectors, and all higher-order correlations are neglected. Denoting $\langle \hat{L}_i \rangle$ by s_i for $i \in x, y, z$, we derive a set of coupled nonlinear equations in terms of s_x , s_y , and s_z .

1. Mathematical Framework

Under the mean-field approximation, a two-point correlator involving the Bloch vectors can be factorized as the product of their individual expectation values. Thus, $\langle \hat{L}_x \hat{L}_z \rangle = \langle \hat{L}_x \rangle \langle \hat{L}_z \rangle = \langle \hat{L}_x \rangle \langle \hat{L}_z \rangle$ and $\langle \hat{L}_y \hat{L}_z \rangle = \langle \hat{L}_y \rangle \langle \hat{L}_z \rangle$ [46]. Writing $c_1 = U_3/2\hbar - U_1/2\hbar - U_2/8\hbar$ and $c_2 = U_1/\hbar - U_2/4\hbar - \epsilon_b/\hbar$, we arrive at the Bloch equations similar to the well-known NMR process [79, 80].

$$\dot{s}_x = 2c_1 s_y s_z + c_2 s_y - \frac{\gamma_z s_x}{2} \quad (14a)$$

$$\begin{aligned} \dot{s}_y &= -2c_1 s_x s_z - c_2 s_x - \frac{\tilde{g}}{\sqrt{2}} (1 + 2s_z - 3s_z^2) \\ &+ \gamma_x (-2s_y + 6s_y s_z) - \frac{\gamma_z s_y}{2} \end{aligned} \quad (14b)$$

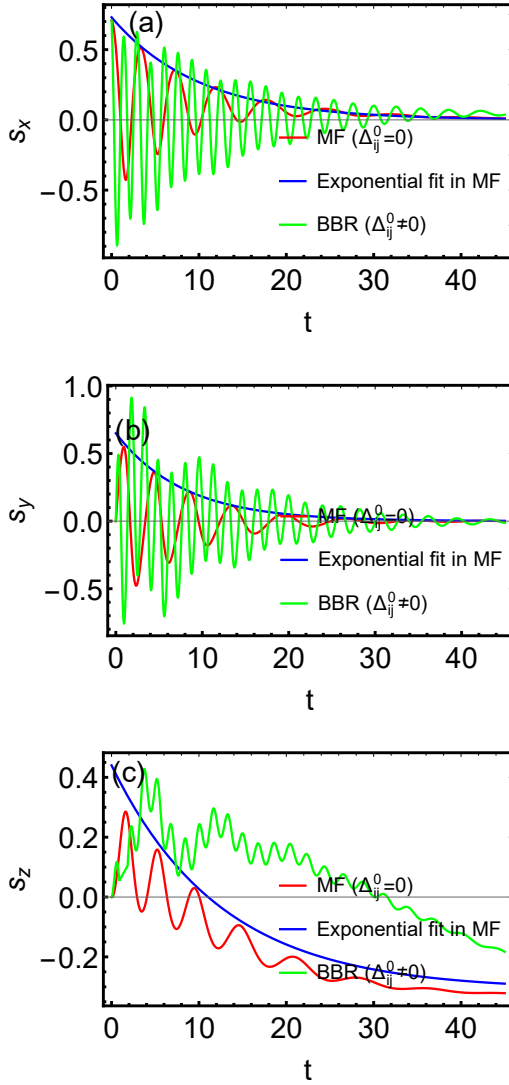


FIG. 3: Mean-field (MF) ($\Delta_{ij}^0 = 0$), beyond mean-field (BBR) ($\Delta_{ij}^0 \neq 0$), and the analytical expression of the relaxation rate in MF are denoted by the (—), (—), and (—) curves, respectively, where Δ_{ij}^0 represents the correlation at $t = 0$. Additionally, the relaxation dynamics of (a) s_x , (b) s_y , and (c) s_z are considered.

$$\dot{s}_z = 2\sqrt{2}\tilde{g}s_y - \gamma_x(1 + 2s_z - 3s_z^2) \quad (14c)$$

Eqs. (14a), (14b), and (14c) can be numerically solved for a given set of initial conditions. To obtain realistic values of the parameters c_1 , c_2 and \tilde{g} , we recall that in Feshbach resonance experiments with ultracold atoms $u_1 = 4\pi\hbar^2 a_{bg}/m_{atom}$, $u_2 = 4\pi\hbar^2 a_{bb}/m_{molecule}$, $u_3 = 4\pi\hbar^2 a_{ab}/\mu$, $g = \sqrt{\mu_{co}}\Delta B u_1$, $\mu = m_a m_b / (m_a + m_b)$, and $\epsilon_b = \mu_{co}(B - B_0)$. Here, a_{bg} and a_{bb} are the background scattering lengths of bosonic atoms and bosonic molecules, and a_{ab} is the scattering length corresponding to atom-molecule interaction. Also, m_{atom} , $m_{molecule}$ and μ are the mass of a bosonic atom, the mass of a bosonic

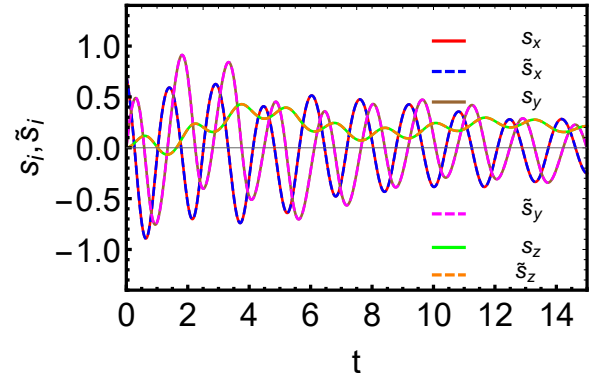


FIG. 4: The Bloch vector components show similar dynamical behavior whether the terms $2s_i s_j$ or $s_i s_j + s_j s_i$ are incorporated into the equations, denoted by s_i and \tilde{s}_i , respectively. The components are represented as follows: $s_x^{2s_i s_j}$ as s_x (—), $s_x^{s_i s_j + s_j s_i}$ as \tilde{s}_x (---), $s_y^{2s_i s_j}$ as s_y (—), $s_y^{s_i s_j + s_j s_i}$ as \tilde{s}_y (---), $s_z^{2s_i s_j}$ as s_z (—), $s_z^{s_i s_j + s_j s_i}$ as \tilde{s}_z (---). Each component is represented by its respective color.

molecule and the reduced mass of a combined bosonic atom-molecule structure respectively. μ_{co} and ΔB represent the magnetic moment and resonance width of the bosonic atom, respectively, where B is the applied magnetic field and B_0 is the resonance position

2. Dynamics of the Bloch Vectors

For numerical solutions, we use the parameters corresponding to Feshbach resonance of ^{87}Rb . Note that ΔB and B_0 have the experimental values 0.21 Gauss and 1007.4 Gauss, respectively [18] for this system. Here, we take $|B - B_0| = 10$ Gauss. In this limit, the values of U_1 , U_2 , U_3 , \tilde{g} and ϵ_b are 1, 2, -1.5, 0.2, and 0.191, respectively [18, 81–83]. We choose γ_x and γ_z to be 10% of \tilde{g} and ϵ_b , respectively. So, the system parameters become: $c_1 = c_2 = -1.5$, $\gamma_x = 0.02$, $\gamma_z = 0.2$. Using Eq. 3, we construct our initial values for the Bloch vector components: $s_x^0 = 0.707$, $s_y^0 = 0$, and $s_z^0 = 0$ (essentially, $\tilde{z} = 0$ and $\tilde{\phi} = 0$). Thus, our starting point is the Josephson state **0** [76, 84] which corresponds to $\tilde{\phi} = 0$.

MF oscillations are plotted using the red-damped curve in Figs. (3a), (3b), and (3c) where Δ_{ij}^0 stands for Δ_{ij} at $t = 0$. From Eq. (14) we obtain the relaxation rate of s_x , s_y , and s_z . For this, we linearize the Eq. (14c) about the stable equilibrium point $(0, 0, -1/3)$. Now, the relaxation rates are the following,

$$\frac{1}{T_x^{\text{MF}}} = \frac{\gamma_z}{2} \quad (15a)$$

$$\frac{1}{T_y^{\text{MF}}} = 2\gamma_x(1 - 3s_z) + \frac{\gamma_z}{2} \quad (15b)$$

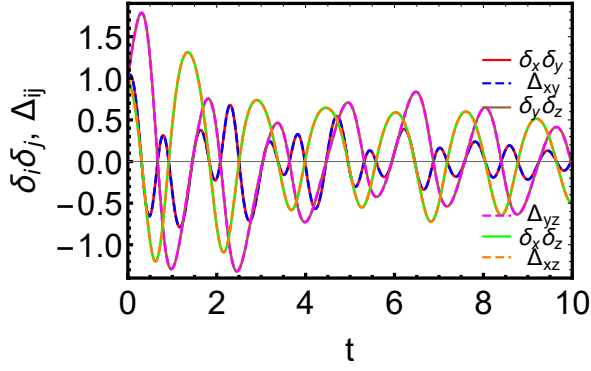


FIG. 5: The quantities δ_i , δ_j , and Δ_{ij} exhibit the same dynamics. Their representations are as follows: $\delta_x \delta_y$ (—), Δ_{xy} (---), $\delta_y \delta_z$ (—), Δ_{yz} (---), $\delta_x \delta_z$ (—), Δ_{xz} (---). Each quantity is denoted by its respective color.

$$\frac{1}{T_z^{\text{MF}}} = 4\gamma_x \quad (15c)$$

The blue curves in Figs. (3a), (3b), and (3c) represent the exponential fits of the damping process in the mean field (MF) approximation. Here, we have modeled s_x , s_y , and s_z as $\approx A_x e^{-t/T_x}$, $\approx A_y e^{-t/T_y}$, and $\approx A_{z1} e^{-t/T_z} - A_{z2}$ against t as obtained from Eq. (15). It should be noted that the peaks of the MF curve (red) fall on this exponential fit (blue) for each s_i . Here, A_x , A_y , and A_{z1} are the exponential fit amplitudes for s_x , s_y , and s_z , respectively. There is a small downward shift A_{z2} in the s_z vs. t plot to capture particle leakage from the M-BEC state to the A-BEC state. For this set of graphs, $A_x = 0.73$, $A_y = 0.65$, $A_{z1} = 0.75$, and $A_{z2} = 0.31$.

In the next subsection (Sec. III B), we discuss the BBGKY or BBR method that successfully incorporates the second moments (variance and covariance) of the bloch vector components in the dynamics. For a quantum system, both the variance and the covariance are non-trivial, and play an important role in the relaxation process.

B. BBR

The mean-field (MF) results are insufficient for accurately describing strongly correlated quantum systems. Therefore, we need to incorporate higher-order expectation values in the dynamical equations. In this section, we present a modified MF theory for the atomic-molecular BEC, by employing up to the second order of the Bogoliubov-Born-Green-Kirkwood-Yvon (BBGKY) hierarchy in the equations of motions. This truncation scheme is often termed the Bogoliubov Backreaction (BBR) method as well.

1. Mathematical Framework

Here, we decompose the expectations of three operators as follows.

$$\begin{aligned} \langle \hat{L}_i \hat{L}_j \hat{L}_k \rangle &\approx \langle \hat{L}_i \hat{L}_j \rangle \langle \hat{L}_k \rangle + \langle \hat{L}_i \rangle \langle \hat{L}_j \hat{L}_k \rangle + \langle \hat{L}_i \hat{L}_k \rangle \langle \hat{L}_j \rangle \\ &\quad - 2 \langle \hat{L}_i \rangle \langle \hat{L}_j \rangle \langle \hat{L}_k \rangle \end{aligned} \quad (16)$$

Moreover, we define the two-point correlation function Δ_{ij} as

$$\Delta_{ij} = \langle \hat{L}_i \hat{L}_j + \hat{L}_j \hat{L}_i \rangle - 2 \langle \hat{L}_i \rangle \langle \hat{L}_j \rangle \quad (17)$$

If $\Delta_{ij} \neq 0$, we enter the BBR regime; otherwise, we stay in the MF regime where $\Delta_{ij} = 0$. In other words, $\Delta_{ij} = 0$ implies that the system remains in the eigenstates of the observable [67, 85]. In terms of 1st and 2nd order moments, Eq. (13) becomes

$$\dot{s}_x = c_1(\Delta_{yz} + 2s_y s_z) + c_2 s_y - \frac{\gamma_z s_x}{2} \quad (18a)$$

$$\begin{aligned} \dot{s}_y = & -c_1(\Delta_{zx} + 2s_z s_x) - c_2 s_x - \frac{\tilde{g}}{\sqrt{2}}(1 + 2s_z - \frac{3}{2}\Delta_{zz} - 3s_z^2) \\ & + \gamma_x(-2s_y + 3\Delta_{yz} + 6s_y s_z) - \frac{\gamma_z s_y}{2} \end{aligned} \quad (18b)$$

$$\dot{s}_z = 2\sqrt{2}\tilde{g}s_y - \gamma_x(1 + 2s_z - \frac{3}{2}\Delta_{zz} - 3s_z^2) \quad (18c)$$

$$\dot{\Delta}_{xx} = 4c_1 s_y \Delta_{zx} + 2(2c_1 s_z + c_2)\Delta_{xy} - \gamma_z \Delta_{xx} \quad (18d)$$

$$\begin{aligned} \dot{\Delta}_{yy} = & \left(-4c_1 s_x - 2\sqrt{2}\tilde{g}(1 - 3s_z) + 12\gamma_x s_y \right) \Delta_{yz} \\ & - 2(2c_1 s_z + c_2)\Delta_{xy} - \left(\gamma_z + 4\gamma_x(1 - 3s_z) \right) \Delta_{yy} \end{aligned} \quad (18e)$$

$$\dot{\Delta}_{zz} = 4\sqrt{2}\tilde{g}\Delta_{yz} - 4\gamma_x(1 - 3s_z)\Delta_{zz} \quad (18f)$$

$$\begin{aligned} \dot{\Delta}_{xy} = & -(2c_1 s_z + c_2)\Delta_{xx} + (2c_1 s_z + c_2)\Delta_{yy} + 2c_1 s_y \Delta_{yz} \\ & + \left(6\gamma_x s_y - 2c_1 s_x - \sqrt{2}\tilde{g}(1 - 3s_z) \right) \Delta_{zx} \\ & - \left(\gamma_z + 2\gamma_x(1 - 3s_z) \right) \Delta_{xy} \end{aligned} \quad (18g)$$

$$\begin{aligned} \dot{\Delta}_{yz} = & \left(-2c_1 s_x - \sqrt{2}\tilde{g}(1 - 3s_z) + 6\gamma_x s_y \right) \Delta_{zz} - (2c_1 s_z + c_2)\Delta_{zx} \\ & + 2\sqrt{2}\tilde{g}\Delta_{yy} - \left(\frac{\gamma_z}{2} + 4\gamma_x(1 - 3s_z) \right) \Delta_{yz} \end{aligned} \quad (18h)$$

$$\begin{aligned} \dot{\Delta}_{zx} = & 2c_1 s_y \Delta_{zz} + (2c_1 s_z + c_2)\Delta_{yz} + 2\sqrt{2}\tilde{g}\Delta_{xy} \\ & - \left(2\gamma_x(1 - 3s_z) + \frac{\gamma_z}{2} \right) \Delta_{zx} \end{aligned} \quad (18i)$$

2. Dynamics of the Bloch vectors

In addition to the initial values specified in Sec. III A 2, we consider variances and covariances $\Delta_{ii}^0 = \Delta_{jj}^0 = 1$ to study the dynamics of s_x , s_y and s_z in Figs. (3a), (3b), and (3c). The green damped oscillatory curves here represent the BBR solutions. It is evident that in the BBR approximation, all three components (s_x , s_y , and s_z) have a longer relaxation time compared to their respective mean-field (MF) counterparts, indicating that a fully correlated system requires more time to relax. However, when certain individual fluctuations (Δ_{ii}^0) or correlations (Δ_{ij}^0) are present, they can lead to longer or shorter relaxation times compared to the MF values, depending on the individual initial conditions.

Additionally, we make two interesting observations. First, if terms like $(s_i s_j + s_j s_i)$ in Eq. (18) are replaced by $2s_i s_j$, the dynamics remains the same. This is demonstrated in Fig. (4), where \tilde{s}_x , \tilde{s}_y , \tilde{s}_z are solutions of the original equations; and s_x , s_y and s_z are solutions of the same set of equations but with $(s_i s_j + s_j s_i)$ substituted by $2s_i s_j$. This shows that we are in the quasi-classical regime, which is consistent with our initial assumption of a large N limit. This is similar to the situation that arises for BEC in a double well [86–91].

Secondly, the terms Δ_{ij} can be written as a product of δ_i and δ_j throughout the course of evolution. This can be illustrated by splitting Δ_{ij}^0 as $\delta_i^0 \delta_j^0$ for each i and j and noting that $\Delta_{ij}(t)$ remains the same as $\delta_i(t) \delta_j(t)$ for all subsequent times. The dynamics of Δ_{xy} , $\delta_x \delta_y$, Δ_{yz} , $\delta_y \delta_z$, Δ_{xz} , and $\delta_x \delta_z$ are represented in Fig. (5). This, again, resembles the situation with two-mode BEC in a double well [62]. The dynamics of δ_x , δ_y , and δ_z here are given by

$$\dot{\delta}_x = 2c_1 s_y \delta_z + (2c_1 s_z + c_2) \delta_y - \frac{\gamma_z}{2} \delta_x \quad (19a)$$

$$\begin{aligned} \dot{\delta}_y = & \left(-2c_1 s_x - \sqrt{2}\tilde{g}(1 - 3s_z) + 6\gamma_x s_y \right) \delta_z - (2c_1 s_z + c_2) \delta_x \\ & - \left(2\gamma_x(1 - 3s_z) + \frac{\gamma_z}{2} \right) \delta_y \end{aligned} \quad (19b)$$

$$\dot{\delta}_z = 2\sqrt{2}\tilde{g}\delta_y - 2\gamma_x(1 - 3s_z)\delta_z \quad (19c)$$

In sec. III B 3 we discuss how the longitudinal (T_z) and transverse (T_{x-y}) relaxation times of s_i vary with a varying Δ_{ii}^0 , $i \in x, y, z$.

3. Longitudinal and transverse relaxation times

In III B 2, we have demonstrated that all Bloch vector components relax more slowly compared to their respective mean-field (MF) counterparts, if correlations and fluctuations are present in all three directions. Next, we focus on the effects of individual variances Δ_{ii}^0 ($i \in x, y, z$). We report the effects of

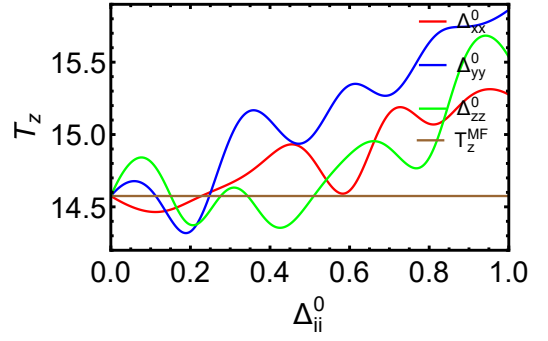


FIG. 6: Effect of activation of variance (Δ_{ii}^0) on longitudinal relaxation time (T_z) where Δ_{xx}^0 (—), Δ_{yy}^0 (—), Δ_{zz}^0 (—) and T_z^{MF} (—) are denoted by their respective colors.

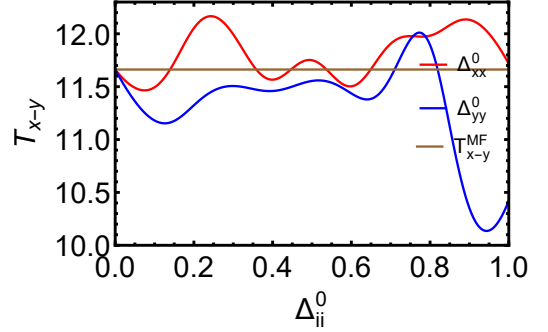


FIG. 7: Effect of activation of variance (Δ_{ii}^0) on transverse relaxation time (T_{x-y}) where Δ_{xx}^0 (—), Δ_{yy}^0 (—) and T_{x-y}^{MF} (—) are denoted by their respective colors. Effect of Δ_{zz}^0 growing on T_{xy} not include here due to rapid fluctuation of s_x , and s_y .

only the variances and not the covariances, because, as shown in III B 2, any Δ_{ij} can be expressed as $\sqrt{\Delta_{ii}\Delta_{jj}}$ ($i, j \in x, y, z$).

Among the relaxation times, the most significant is the longitudinal relaxation time T_z that sets the scale for the population imbalance between the atomic and molecular modes to approach its equilibrium value. We observe that this T_z increases with the activation of each Δ_{ii}^0 as shown in Fig. (6).

In Eq. (15), the decay rates of the components s_x , s_y differ, so the decay rate in the anisotropic transverse plane can be characterized by the harmonic mean [92, 93]:

$$T_{x-y} = \frac{2T_x T_y}{T_x + T_y} \quad (20)$$

Greater correlations lead to more coherent oscillations in the equatorial plane, i.e., s_x and s_y persist longer, resulting in an increased coherence time. This is shown in Fig. (7): we see that when Δ_{xx}^0 increases, T_{x-y} also increases. In contrast, an increase in Δ_{yy}^0 reduces T_{x-y} . We could not include T_{x-y} vs. Δ_{zz}^0 curve in this plot due to rapid fluctuations of s_x , and s_y . In the next section (Sec. IV), we try to justify these results and put some physical insight behind why depending on the correlations present, the longitudinal and transverse relaxation

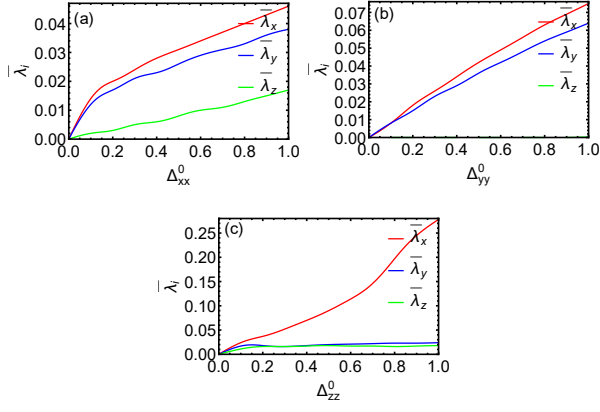


FIG. 8: time-averaged structural or elliptic noise ($\bar{\lambda}_i$) vs. variances (Δ_{ii}^0) for $\bar{\lambda}_x$ (—), $\bar{\lambda}_y$ (—), and $\bar{\lambda}_z$ (—) along s_x , s_y , and s_z axis when (a) Δ_{xx}^0 , (b) Δ_{yy}^0 , and (c) Δ_{zz}^0 are activated.

times either get prolonged or shortened.

IV. COHERENCE DOMINATED RELAXATION TIME

In this section, we try to provide physical arguments to explain the results obtained in Sec. III, especially in the presence of fluctuations and correlations. To achieve this, we take time-averages of relevant physical quantities. For this, we take the time average of any operator \hat{A} , such as $\langle \hat{A} \rangle_t = \bar{A}$, over the time (in our unit $t = 0$ to $t = 50$) during which the dynamics persists. Now, temporal averages best describe the system either under equilibrium configurations, or under non-equilibrium steady-state conditions. We understand that our system belongs to neither of these two classes and deals with a transient phenomenon (relaxation dynamics) instead. The reason we still define time averages and use them in physical interpretations is that we simply wish to capture the dominant physical traits as the system journeys back to equilibrium, and a time-averaged description works best for that purpose. Since all calculations have been performed considering weak noise, the system can be treated in the linear response regime. Thus, the response of the system to the small noise is still governed by equilibrium fluctuations. However, nowhere in this section has the time average been equated with the ensemble average, so the question of ergodicity (or the breaking thereof) does not even arise. The time-averages that we talk about are simply indicators of the gross overall behaviors of the atoms and molecules and their approach to a steady state.

In Sec. IV A, we described the effect of elliptic noise as a squeezed state, which enhances coherence.

A. Elliptic noise: Squeezed state

One of the key features that emerges is that in the presence of fluctuations about the equilibrium values of the Bloch

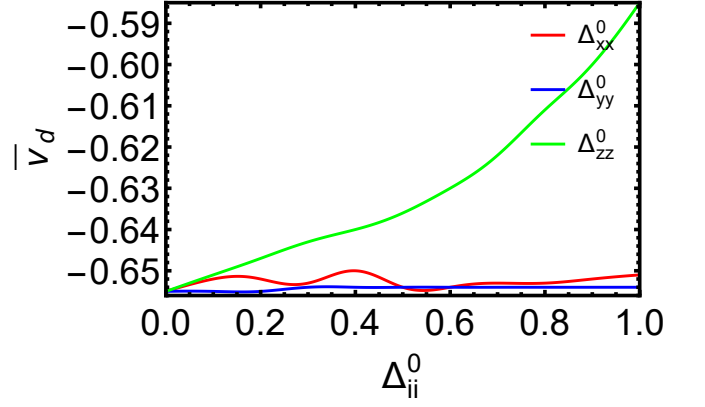


FIG. 9: variance (Δ_{ii}^0) motivated time-averaged drift speed (\bar{v}_d) where the following correlations are represented by their respective colors for : Δ_{xx}^0 (—), Δ_{yy}^0 (—), and Δ_{zz}^0 (—)

vectors, the relaxation time typically increases, especially for s_z . It is sort of counterintuitive because the fluctuations could help the system relax faster by facilitating transitions between different configurations. To justify our findings, we present the time-averaged structure matrix, or the real-symmetric covariance matrix, defined as

$$\bar{\Delta}_{ij} = \begin{pmatrix} \bar{\Delta}_{xx} & \bar{\Delta}_{xy} & \bar{\Delta}_{xz} \\ \bar{\Delta}_{xy} & \bar{\Delta}_{yy} & \bar{\Delta}_{yz} \\ \bar{\Delta}_{xz} & \bar{\Delta}_{yz} & \bar{\Delta}_{zz} \end{pmatrix} \quad (21)$$

whose eigenvalues represent the variances along the principal axes. When two of the eigenvalues of the covariance matrix are nearly equal and the third differs significantly, the noise distribution assumes an ellipsoidal shape [78, 94], indicating structured fluctuations [92], where one quadrature is expanded while the other is reduced. Such anisotropic noise leads to the formation of squeezed states. It is this structured noise that enhances the robustness of the non-equilibrium system by suppressing specific decoherence channels, thereby increasing the relaxation time or prolonging coherence. In our system, increasing Δ_{xx}^0 and Δ_{yy}^0 causes $\bar{\lambda}_x$ and $\bar{\lambda}_y$ to become nearly equal, while $\bar{\lambda}_z$ remains significantly smaller as shown in Figs. (8a) and (8b). When Δ_{zz}^0 increases, $\bar{\lambda}_y$ and $\bar{\lambda}_z$ become nearly equal, and $\bar{\lambda}_x$ grows substantially, as illustrated in Fig. (8c). In both cases, the noise exhibits an elliptic structure, suggesting that the system's dynamics becomes increasingly constrained, and therefore, relaxation occurs more slowly.

B. Other time-averaged quantities as indicators of coherence

So far, we have observed that the longitudinal relaxation time increases under the influence of any type of fluctuations. On the contrary, the transverse relaxation time increases with an increasing Δ_{xx}^0 or Δ_{zz}^0 , and decreases with an increasing Δ_{yy}^0 . Now, we study the effect of correlations on a few relevant

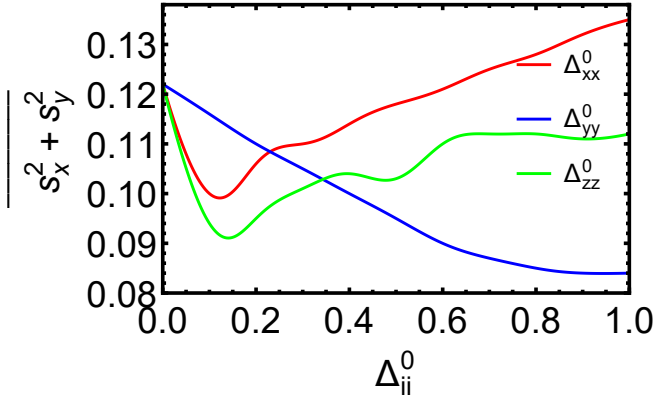


FIG. 10: Time-averaged fringe-visibility ($\overline{s_x^2 + s_y^2}$) dominated by fluctuations where the following variances (Δ_{ii}^0) are represented by their respective colors for : Δ_{xx}^0 (—), Δ_{yy}^0 (—), and Δ_{zz}^0 (—)

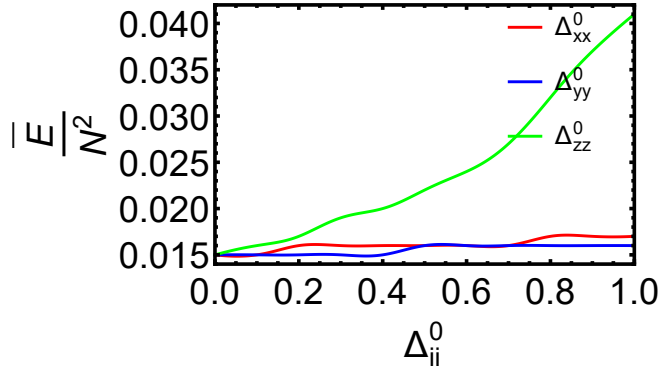


FIG. 11: time-averaged Phase-entanglement (\bar{E}) controlled by Δ_{ii}^0 where the following correlations are represented by their respective colors for : Δ_{xx}^0 (—), Δ_{yy}^0 (—), and Δ_{zz}^0 (—)

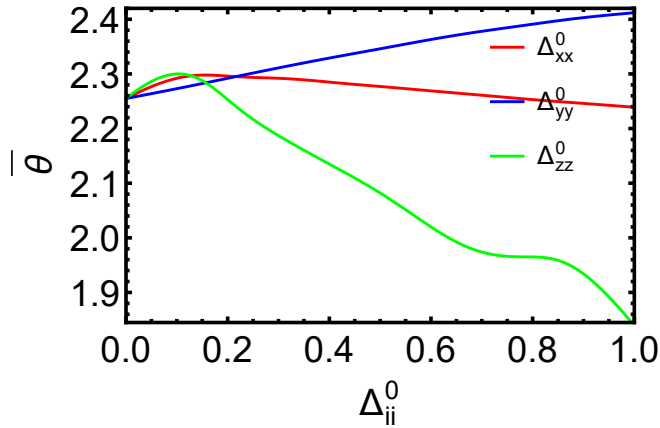


FIG. 12: time-averaged polar angle ($\bar{\theta}$) controlled by Δ_{ii}^0 where the following variances are represented by their respective colors for : Δ_{xx}^0 (—), Δ_{yy}^0 (—), and Δ_{zz}^0 (—)

physical quantities, and try to tally the findings with the trends that arise in the relaxation process. Three such quantities that we address here are (i) drift speed, (ii) fringe visibility, (iii) EPR entanglement, and (iv) the polar angle of the Bloch vector.

1. Drift speed

We notice that the drift speed decreases [95] with an increase in structured quantum noise [96] as shown in Fig. (6). Note that the drift speed, defined as \dot{s}_z , represents the tunneling speed between the molecular and atomic states.

2. Fringe visibility

This quantity can be captured in time-of-flight interference experiments [97]. We have studied the fringe-visibility of our system using density matrix formalism. Here, the density matrix can be expressed as [78, 98]:

$$\hat{\rho} = \frac{I + \sigma_j s_j}{2}, \quad \text{where } j \in x, y, z \quad (22)$$

Here, σ_j are (2×2) Pauli matrices. In matrix form, Eq. (22) becomes:

$$\hat{\rho} = \frac{1}{2} \begin{pmatrix} 1 + s_z & s_x - i s_y \\ s_x + i s_y & 1 - s_z \end{pmatrix} \quad (23)$$

the magnitude of this off-diagonal element, s_{\parallel} is called fringe-visibility. We calculate the evolution of the time-averaged transverse component ($\bar{s}_{\parallel} = \overline{s_x^2 + s_y^2}$) [99, 100] with increasing initial variances. We observe that $\bar{s_x^2 + s_y^2}$ increases with an increasing Δ_{xx}^0 or Δ_{zz}^0 , and decreases with a decreasing Δ_{yy}^0 . Since coherence corresponds to the magnitude of the off-diagonal elements of the density matrix, the dephasing mechanism can be identified when the average projection length (S_{\parallel}) shrinks. So clearly, a growth in the fringe visibility implies a larger relaxation time, and a decay in the visibility indicates a faster relaxation process, as evident from Figs. (7) and (10).

Actually, fringe visibility is the amplitude of population oscillation.

3. EPR entanglement

The Einstein-Podolski-Rosen (EPR) entanglement or phase entanglement measurement [101] E is another key element to study the coherence of the system, which is defined as,

$$E = \langle \hat{L}_+ \hat{L}_- \rangle - \langle 2\hat{n}_b \rangle \langle \hat{n}_a \rangle \quad (24a)$$

which recasts as large N limit

$$\frac{E}{N^2} \approx \frac{2s_z^2 + \Delta_{zz}}{8} \quad (24b)$$

where, $\hat{L}_+ = \hat{a}^\dagger \hat{a}^\dagger \hat{b}$, and $\hat{L}_- = \hat{b}^\dagger \hat{a} \hat{a}$. From Fig. (11), we observe that E increases when either Δ_{xx}^0 or Δ_{zz}^0 increases. On the other hand, if Δ_{yy}^0 increases, then E slightly decreases: again, consistent with the corresponding relaxation processes.

4. Variation of the polar angle

In Sec. III B 2 and Sec. IV B, it has been discussed how introduction of the variances Δ_{xx} and Δ_{zz} influence the system in a similar way, while the impact of Δ_{yy} is exactly opposite. This can be justified by studying the polar angle (θ) between s_z axis and \mathbf{s} in Fig. (2). This θ can be defined as,

$$\theta = \cos^{-1} \frac{s_z}{|\mathbf{s}|} \quad (25)$$

Its variation with each Δ_{ii}^0 is shown in Fig. (12). We find that the time-averaged polar angle lies in 2nd quadrant, i.e., $\frac{\pi}{2} < \bar{\theta} < \pi$, which means, if $\bar{\theta}$ decreases then the precession cone becomes wider like a classical top motion [102]. If the radius of precession cone ($s_{||}$) increases then coherence also increases because, $s_{||}$ is nothing but the square root of the Fringe Visibility. If θ moves from π to $\frac{\pi}{2}$, then $s_x \approx \cos \theta$ remains while $s_y \approx \sin \theta$ becomes negative. Thus, in our regime of interest, s_x , and s_y bear opposite signs.

In the equatorial plane ($s_z = 0$), $s_{||}$ reaches its maximum because [47]

$$s_x^2 + s_y^2 = \frac{(1 + s_z)(1 - s_z)^2}{2} \quad (26)$$

If we add small fluctuation on eac s_i as δs_i ($i \in x, y, z$) then Eq. (26) becomes

$$s_x \delta s_x + s_y \delta s_y = -\frac{(1 - s_z)(1 + 3s_z)\delta s_z}{2} \quad (27)$$

Since $\bar{\theta}$ remains in 2nd quadrant, $s_x < 0$ and $s_y > 0$ in Eq. (27). Thus, δs_x and δs_z carry same signs, and that of δs_y is the opposite. As a result, the impact of Δ_{xx} and Δ_{zz} are closer, while that of Δ_{yy} is the opposite. Therefore, in Figs. (7), (10), (11), and (12) an activation of Δ_{yy} works in opposite of an activation of Δ_{xx} and Δ_{zz} .

V. SUMMARY AND CONCLUSION

In this work, we have studied a system of bosonic atoms coupled via a Feshbach resonance, capable of forming bosonic dimers. We have corrupted both the Feshbach detuning and the Feshbach coupling by Gaussian white noise, and studied the corresponding relaxation dynamics. We have described the system in a Bloch sphere representation. where (\hat{L}_z) denotes the population difference between atomic and molecular Bose-Einstein condensates (BECs), and \hat{L}_x and \hat{L}_y represent the real and imaginary parts of the coherences, respectively.

We adopted two methods for studying the dynamics. In the mean-field (MF) approach, only the mean values are considered: $s_i = \langle \hat{L}_i \rangle$. In contrast, the Bogoliubov Backreaction (BBR) method accounts for both the mean and the second moments i.e., variances (Δ_{ii}^0) and covariances (Δ_{ij}^0).

Since the system contains particle-conserving noise (i.e., $\dot{N} = 0$), the relaxation times of both polarization (s_{\perp}) and coherence ($s_{||}$) are characterized by the longitudinal (T_z) and transverse (T_{x-y}) relaxation times, respectively. Here, we observe that T_z always increases under the influence of any rising Δ_{ii}^0 . However, T_{x-y} increases when Δ_{xx}^0 and Δ_{zz}^0 increase, whereas an increase in Δ_{yy}^0 drives the system towards a smaller T_{x-y} . We found a connection of this result with the behaviour of several related physical quantities : (i) drift speed (v_d) (ii) fringe visibility ($s_x^2 + s_y^2$), (iii) EPR entanglement (E), and (iv) polar angle (θ).

In the present manuscript, the influence of the variances Δ_{ii}^0 and covariances Δ_{ij}^0 of the Bloch vector on the system evolution is reported only. However, Feshbach detuning and initial polarization also play important roles in controlling the system dynamics. we intend to investigate these two aspects in future. Moreover, another interesting phenomenon observed in certain quantum system is that a certain amount of noise [73, 103, 104] can enhance coherence a phenomenon known as coherence resonance. A study of this coherence resonance for the atomic-molecular condensates is also on our cards.

* avinaba.mukherjee@rediffmail.com

† rdphy@caluniv.ac.in

- [1] P. Naidon, E. Tiesinga, and P. S. Julienne, Two-body transients in coupled atomic-molecular bose-einstein condensates, *Physical review letters* **100**, 093001 (2008).
- [2] M. Holland, J. Park, and R. Walser, Formation of pairing fields in resonantly coupled atomic and molecular bose-einstein condensates, *Physical Review Letters* **86**, 1915 (2001).
- [3] M. Gupta and K. R. Dastidar, Control of the dynamics of coupled atomic-molecular bose-einstein condensates: Modified gross-pitaevskii approach, *Physical Review A Atomic, Molecular, and Optical Physics* **80**, 043618 (2009).
- [4] G.-R. Jin, C. K. Kim, and K. Nahm, Quantum dynamics and statistical properties of atom-molecule bose-einstein condensates, *Physical Review A Atomic, Molecular, and Optical Physics* **72**, 045602 (2005).
- [5] T. Köhler, T. Gasenzer, and K. Burnett, Microscopic theory of atom-molecule oscillations in a bose-einstein condensate, *Physical Review A* **67**, 013601 (2003).
- [6] E. Braaten and H.-W. Hammer, Enhanced dimer relaxation in an atomic and molecular bose-einstein condensate, *Physical Review A Atomic, Molecular, and Optical Physics* **70**, 042706 (2004).
- [7] M. Mackie, A. Collin, and J. Javanainen, Comment on “stimulated raman adiabatic passage from an atomic to a molecular bose-einstein condensate”, *Physical Review A—Atomic, Molecular, and Optical Physics* **71**, 017601 (2005).
- [8] P. Drummond, K. Kheruntsyan, D. Heinzen, and R. Wynar, Stimulated raman adiabatic passage from an atomic to a

- molecular bose-einstein condensate, *Physical Review A* **65**, 063619 (2002).
- [9] B. J. Cusack, T. J. Alexander, E. A. Ostrovskaya, and Y. S. Kivshar, Existence and stability of coupled atomic-molecular bose-einstein condensates, *Physical Review A* **65**, 013609 (2001).
 - [10] A. Vardi, V. Yurovsky, and J. Anglin, Quantum effects on the dynamics of a two-mode atom-molecule bose-einstein condensate, *Physical Review A* **64**, 063611 (2001).
 - [11] J. Hope and M. Olsen, Quantum superchemistry: Dynamical quantum effects in coupled atomic and molecular bose-einstein condensates, *Physical Review Letters* **86**, 3220 (2001).
 - [12] J.-J. Zhu and X. Chen, Fast-forward scaling of atom-molecule conversion in bose-einstein condensates, *Physical Review A* **103**, 023307 (2021).
 - [13] A. P. Tonel, C. C. N. Kuhn, G. Santos, A. Foerster, I. Roditi, and Z. V. T. Santos, Classical and quantum analysis of a heterotriatomic molecular bose-einstein-condensate model, *Physical Review A Atomic, Molecular, and Optical Physics* **79**, 013624 (2009).
 - [14] M. Mackie, A. Collin, and J. Javanainen, Comment on “stimulated raman adiabatic passage from an atomic to a molecular bose-einstein condensate”, *Physical Review A Atomic, Molecular, and Optical Physics* **71**, 017601 (2005).
 - [15] T. G. Vaughan, K. Kheruntsyan, and P. Drummond, Three-dimensional solitons in coupled atomic-molecular bose-einstein condensates, *Physical Review A Atomic, Molecular, and Optical Physics* **70**, 063611 (2004).
 - [16] K. Kheruntsyan and P. Drummond, Quantum correlated twin atomic beams via photodissociation of a molecular bose-einstein condensate, *Physical Review A* **66**, 031602 (2002).
 - [17] E. Timmermans, P. Tommasini, M. Hussein, and A. Kerman, Feshbach resonances in atomic bose-einstein condensates, *Physics Reports* **315**, 199 (1999).
 - [18] T. Köhler, K. Góral, and P. S. Julienne, Production of cold molecules via magnetically tunable feshbach resonances, *Reviews of modern physics* **78**, 1311 (2006).
 - [19] M. Pigneur, T. Berrada, M. Bonneau, T. Schumm, E. Demler, and J. Schmiedmayer, Relaxation to a phase-locked equilibrium state in a one-dimensional bosonic josephson junction, *Physical review letters* **120**, 173601 (2018).
 - [20] R. Gerritsma, A. Negretti, H. Doerk, Z. Idziaszek, T. Calarco, and F. Schmidt-Kaler, Bosonic josephson junction controlled by a single trapped ion, *Physical Review Letters* **109**, 080402 (2012).
 - [21] T. Betz, S. Manz, R. Bücker, T. Berrada, C. Koller, G. Kazakov, I. E. Mazets, H.-P. Stimming, A. Perrin, T. Schumm, *et al.*, Two-point phase correlations of a one-dimensional bosonic josephson junction, *Physical review letters* **106**, 020407 (2011).
 - [22] E. Boukobza, M. G. Moore, D. Cohen, and A. Vardi, Nonlinear phase dynamics in a driven bosonic josephson junction, *Physical review letters* **104**, 240402 (2010).
 - [23] M. Albiez, R. Gati, J. Fölling, S. Hunsmann, M. Cristiani, and M. K. Oberthaler, Direct observation of tunneling and nonlinear self-trapping in a single bosonic josephson junction, *Physical review letters* **95**, 010402 (2005).
 - [24] J. Tian, H. Qiu, G. Wang, Y. Chen, and L.-b. Fu, Measure synchronization in a two-species bosonic josephson junction, *Physical Review E—Statistical, Nonlinear, and Soft Matter Physics* **88**, 032906 (2013).
 - [25] S. Wimberger, G. Manganelli, A. Brollo, and L. Salasnich, Finite-size effects in a bosonic josephson junction, *Physical Review A* **103**, 023326 (2021).
 - [26] M. Pigneur and J. Schmiedmayer, Analytical pendulum model for a bosonic josephson junction, *Physical Review A* **98**, 063632 (2018).
 - [27] J. Schurer, R. Gerritsma, P. Schmelcher, and A. Negretti, Impact of many-body correlations on the dynamics of an ion-controlled bosonic josephson junction, *Physical Review A* **93**, 063602 (2016).
 - [28] K. Sakmann, A. I. Streltsov, O. E. Alon, and L. S. Cederbaum, Universality of fragmentation in the schrödinger dynamics of bosonic josephson junctions, *Physical Review A* **89**, 023602 (2014).
 - [29] P. Buonsante, R. Burioni, E. Vescovi, and A. Vezzani, Quantum criticality in a bosonic josephson junction, *Physical Review A Atomic, Molecular, and Optical Physics* **85**, 043625 (2012).
 - [30] M. Lapert, G. Ferrini, and D. Sugny, Optimal control of quantum superpositions in a bosonic josephson junction, *Physical Review A Atomic, Molecular, and Optical Physics* **85**, 023611 (2012).
 - [31] M. Chuchem, K. Smith-Mannschott, M. Hiller, T. Kottos, A. Vardi, and D. Cohen, Quantum dynamics in the bosonic josephson junction, *Physical Review A Atomic, Molecular, and Optical Physics* **82**, 053617 (2010).
 - [32] K. Sakmann, A. I. Streltsov, O. E. Alon, and L. S. Cederbaum, Quantum dynamics of attractive versus repulsive bosonic josephson junctions: Bose-hubbard and full-hamiltonian results, *Physical Review A Atomic, Molecular, and Optical Physics* **82**, 013620 (2010).
 - [33] G. Mazzarella, L. Salasnich, A. Parola, and F. Toigo, Coherence and entanglement in the ground state of a bosonic josephson junction: From macroscopic schrödinger cat states to separable fock states, *Physical Review A Atomic, Molecular, and Optical Physics* **83**, 053607 (2011).
 - [34] X. Jia, W. Li, and J. Liang, Nonlinear correction to the boson josephson-junction model, *Physical Review A Atomic, Molecular, and Optical Physics* **78**, 023613 (2008).
 - [35] M. Abad, M. Guilleumas, R. Mayol, M. Pi, and D. M. Jezek, Phase slippage and self-trapping in a self-induced bosonic josephson junction, *Physical Review A Atomic, Molecular, and Optical Physics* **84**, 035601 (2011).
 - [36] F. Binanti, K. Furutani, and L. Salasnich, Dissipation and fluctuations in elongated bosonic josephson junctions, *Physical Review A* **103**, 063309 (2021).
 - [37] K. Kasamatsu, Uniformly frustrated bosonic josephson-junction arrays, *Physical Review A Atomic, Molecular, and Optical Physics* **79**, 021604 (2009).
 - [38] G. Szirmai, G. Mazzarella, and L. Salasnich, Tunneling dynamics of bosonic josephson junctions assisted by a cavity field, *Physical Review A* **91**, 023601 (2015).
 - [39] Y. Huang, Q.-S. Tan, L.-B. Fu, and X. Wang, Coherence dynamics of a two-mode bose-einstein condensate coupled with the environment, *Physical Review A* **88**, 063642 (2013).
 - [40] L. Pitaevskii and S. Stringari, Thermal vs quantum decoherence in double well trapped bose-einstein condensates, *Physical Review Letters* **87**, 180402 (2001).
 - [41] W. Wang, L. Fu, and X. Yi, Effect of decoherence on the dynamics of bose-einstein condensates in a double-well potential, *Physical Review A Atomic, Molecular, and Optical Physics* **75**, 045601 (2007).
 - [42] A. Burchianti, F. Scazza, A. Amico, G. Valtolina, J. Seman, C. Fort, M. Zaccanti, M. Inguscio, and G. Roati, Connecting dissipation and phase slips in a josephson junction between fermionic superfluids, *Physical review letters* **120**, 025302 (2018).

- (2018).
- [43] J.-F. Mennemann, I. E. Mazets, M. Pigneur, H. P. Stimming, N. J. Mauser, J. Schmiedmayer, and S. Erne, Relaxation in an extended bosonic josephson junction, *Physical Review Research* **3**, 023197 (2021).
 - [44] R. Gati and M. K. Oberthaler, A bosonic josephson junction, *Journal of Physics B: Atomic, Molecular and Optical Physics* **40**, R61 (2007).
 - [45] D. Stefanatos and E. Paspalakis, Relaxation dynamics in a stochastic bosonic josephson junction, *Physics Letters A* **383**, 2370 (2019).
 - [46] Y. Khodorkovsky, G. Kurizki, and A. Vardi, Decoherence and entanglement in a bosonic josephson junction: Bose-enhanced quantum zeno control of phase diffusion, *Physical Review A Atomic, Molecular, and Optical Physics* **80**, 023609 (2009).
 - [47] H. Shen, X.-M. Xiu, and X. Yi, Atom-molecule-conversion system subject to phase noises, *Physical Review A Atomic, Molecular, and Optical Physics* **87**, 063613 (2013).
 - [48] F. Van Abeelen and B. Verhaar, Time-dependent feshbach resonance scattering and anomalous decay of a na bose-einstein condensate, *Physical review letters* **83**, 1550 (1999).
 - [49] E. A. Donley, N. R. Claussen, S. T. Thompson, and C. E. Wieman, Atom-molecule coherence in a bose-einstein condensate, *Nature* **417**, 529 (2002).
 - [50] N. R. Claussen, S. Kokkelmans, S. T. Thompson, E. A. Donley, E. Hodby, and C. Wieman, Very-high-precision bound-state spectroscopy near a 85 rb feshbach resonance, *Physical Review A* **67**, 060701 (2003).
 - [51] N. R. Claussen, S. Kokkelmans, S. T. Thompson, E. A. Donley, E. Hodby, and C. Wieman, Very-high-precision bound-state spectroscopy near a 85 rb feshbach resonance, *Physical Review A* **67**, 060701 (2003).
 - [52] G. Santos, A. Tonel, A. Foerster, and J. Links, Classical and quantum dynamics of a model for atomic-molecular bose-einstein condensates, *Physical Review A Atomic, Molecular, and Optical Physics* **73**, 023609 (2006).
 - [53] G.-R. Jin, C. K. Kim, and K. Nahm, Quantum dynamics and statistical properties of atom-molecule bose-einstein condensates, *Physical Review A Atomic, Molecular, and Optical Physics* **72**, 045602 (2005).
 - [54] G. Santos, A. Foerster, J. Links, E. Mattei, and S. R. Dahmen, Quantum phase transitions in an interacting atom-molecule boson model, *Physical Review A Atomic, Molecular, and Optical Physics* **81**, 063621 (2010).
 - [55] J. Li, D.-F. Ye, C. Ma, L.-B. Fu, and J. Liu, Role of particle interactions in a many-body model of feshbach-molecule formation in bosonic systems, *Physical Review A Atomic, Molecular, and Optical Physics* **79**, 025602 (2009).
 - [56] A. Auerbach, *Interacting Electrons and Quantum Magnetism* (Springer Verlag, 1994).
 - [57] J. N. J. Sakurai, *Modern Quantum Mechanics*, 2nd ed. (Addison Wesley Publishing Company, 2011).
 - [58] J. Liu, B. Liu, and L.-B. Fu, Many-body effects on nonadiabatic feshbach conversion in bosonic systems, *Physical Review A Atomic, Molecular, and Optical Physics* **78**, 013618 (2008).
 - [59] B. Cui, L. Wang, and X. Yi, Atom-molecule conversion with particle losses, *Physical Review A Atomic, Molecular, and Optical Physics* **85**, 013618 (2012).
 - [60] A. Motohashi and T. Nikuni, Particle-localized ground state of atom-molecule bose-einstein condensates in a double-well potential, *Physical Review A Atomic, Molecular, and Optical Physics* **82**, 033631 (2010).
 - [61] J. T. Mendonca and H. Tercas, *Physics of Ultra-cold Matter* (Springer, 2013).
 - [62] A. Vardi and J. Anglin, Bose-einstein condensates beyond mean field theory: Quantum backreaction as decoherence, *Physical Review Letters* **86**, 568 (2001).
 - [63] Y. Band, I. Tikhonenkov, and A. Vardi, Adiabatic molecular dynamics: two-body and many-body aspects, *Molecular Physics* **106**, 349 (2008).
 - [64] E. Pazy, I. Tikhonenkov, Y. Band, M. Fleischhauer, and A. Vardi, Nonlinear adiabatic passage from fermion atoms to boson molecules, *Physical review letters* **95**, 170403 (2005).
 - [65] I. Tikhonenkov, E. Pazy, Y. Band, M. Fleischhauer, and A. Vardi, Many-body effects on adiabatic passage through feshbach resonances, *Physical Review A Atomic, Molecular, and Optical Physics* **73**, 043605 (2006).
 - [66] M. Frimmer and L. Novotny, The classical bloch equations, *American Journal of Physics* **82**, 947 (2014).
 - [67] P. C. Deshmukh, *Quantum Mechanics*, 1st ed. (Cambridge University Press, 2023).
 - [68] B. Liu, L.-B. Fu, and J. Liu, Shapiro-like resonance in ultracold molecule production via an oscillating magnetic field, *Physical Review A Atomic, Molecular, and Optical Physics* **81**, 013602 (2010).
 - [69] K. E. Strecker, G. B. Partridge, and R. G. Hulet, Conversion of an atomic fermi gas to a long-lived molecular bose gas, *Physical review letters* **91**, 080406 (2003).
 - [70] J. Liu, L.-B. Fu, B. Liu, and B. Wu, Role of particle interactions in the feshbach conversion of fermionic atoms to bosonic molecules, *New Journal of Physics* **10**, 123018 (2008).
 - [71] C. W. Gardiner, *Handbook of stochastic methods for physics, chemistry and the natural sciences*, Springer series in synergetics (1985).
 - [72] M. Schlosshauer, *Decoherence and the Quantum to Classical Transition* (Springer, 2007).
 - [73] D. Witthaut, F. Trimborn, and S. Wimberger, Dissipation induced coherence of a two-mode bose-einstein condensate, *Physical review letters* **101**, 200402 (2008).
 - [74] J. Anglin, Cold, dilute, trapped bosons as an open quantum system, *Physical review letters* **79**, 6 (1997).
 - [75] J. Ruostekoski and D. F. Walls, Bose-einstein condensate in a double-well potential as an open quantum system, *Physical Review A* **58**, R50 (1998).
 - [76] A. K. Saha, D. S. Ray, and B. Deb, Phase diffusion and fluctuations in a dissipative bose-josephson junction, *Physical Review E* **107**, 034141 (2023).
 - [77] V. Balakrishnan, *Elements of nonequilibrium statistical mechanics*, Vol. 3 (Springer, 2008).
 - [78] C. Gardiner and P. Zoller, *Quantum noise: a handbook of Markovian and non-Markovian quantum stochastic methods with applications to quantum optics* (Springer Science & Business Media, 2004).
 - [79] F. Bloch, Nuclear induction, *Physical review* **70**, 460 (1946).
 - [80] L. Viola, E. Fortunato, S. Lloyd, C.-H. Tseng, and D. Cory, Stochastic resonance and nonlinear response using nmr spectroscopy, *Physical Review Letters* **84**, 5466 (2000).
 - [81] K. E. Strecker, G. B. Partridge, and R. G. Hulet, Conversion of an atomic fermi gas to a long-lived molecular bose gas, *Physical review letters* **91**, 080406 (2003).
 - [82] G.-R. Jin, C. K. Kim, and K. Nahm, Quantum dynamics and statistical properties of atom-molecule bose-einstein condensates, *Physical Review A Atomic, Molecular, and Optical Physics* **72**, 045602 (2005).
 - [83] J. Liu, L.-B. Fu, B. Liu, and B. Wu, Role of particle interactions in the feshbach conversion of fermionic atoms to bosonic molecules, *New Journal of Physics* **10**, 123018 (2008).

- [84] I. Marino, S. Raghavan, S. Fantoni, S. Shenoy, and A. Smerzi, Bose-condensate tunneling dynamics: Momentum-shortened pendulum with damping, *Physical Review A* **60**, 487 (1999).
- [85] A. I. Yoshihisa Yamamoto, *Mesoscopic Quantum Optics* (Wiley, 1999).
- [86] E.-M. Graefe, M. Höning, and H. J. Korsch, Classical limit of non-hermitian quantum dynamics—a generalized canonical structure, *Journal of Physics A: Mathematical and Theoretical* **43**, 075306 (2010).
- [87] E.-M. Graefe, H. J. Korsch, and A. E. Niederle, Quantum-classical correspondence for a non-hermitian bose-hubbard dimer, *Physical Review A Atomic, Molecular, and Optical Physics* **82**, 013629 (2010).
- [88] E. M. Graefe, H. Korsch, and A. Niederle, Mean-field dynamics of a non-hermitian bose-hubbard dimer, *Physical review letters* **101**, 150408 (2008).
- [89] J. Pi, F. Chen, Q. Liu, L. You, and R. Lü, The dynamics of an open bose–hubbard dimer with effective asymmetric coupling, *The European Physical Journal B* **97**, 26 (2024).
- [90] G. V. Soares and J. P. de Faria, Dominant lyapunov mapping in phase and parameters spaces corresponding to the thermodynamic limit of the two-mode bose–hubbard model applied to the control of collapses of josephson oscillations, *The European Physical Journal D* **77**, 14 (2023).
- [91] E.-M. Graefe and C. Liverani, Mean-field approximation for a bose–hubbard dimer with complex interaction strength, *Journal of Physics A: Mathematical and Theoretical* **46**, 455201 (2013).
- [92] M. O. Scully and M. S. Zubairy, *Quantum Optics* (Cambridge University Press, 1997).
- [93] C. P. Slichter, *Principles of Magnetic Resonance*, 3rd ed. (Springer, 1989).
- [94] M. Kitagawa and M. Ueda, Squeezed spin states, *Physical Review A* **47**, 5138 (1993).
- [95] Y. Khodorkovsky, G. Kurizki, and A. Vardi, Decoherence and entanglement in a bosonic josephson junction: Bose-enhanced quantum zeno control of phase diffusion, *Physical Review A Atomic, Molecular, and Optical Physics* **80**, 023609 (2009).
- [96] H. P. Breuer and F. Petruccione, *The Theory of Open Quantum Systems* (Oxford University Press, 2002).
- [97] K. H. Bennemann and J. B. Ketterson, *Novel Superfluids*, Vol. 2 (Oxford University Press, 2014).
- [98] M. A. Nielsen and I. L. Chuang, *Quantum Computation and Quantum Information* (Cambridge University Press, 2000).
- [99] Y. Hao and Q. Gu, Dynamics of two-component bose-einstein condensates coupled with the environment, *Physical Review A Atomic, Molecular, and Optical Physics* **83**, 043620 (2011).
- [100] M. Chuchem, K. Smith-Mannschott, M. Hiller, T. Kottos, A. Vardi, and D. Cohen, Quantum dynamics in the bosonic josephson junction, *Physical Review A Atomic, Molecular, and Optical Physics* **82**, 053617 (2010).
- [101] T. Pudlik, H. Hennig, D. Witthaut, and D. K. Campbell, Dynamics of entanglement in a dissipative bose-hubbard dimer, *Physical Review A Atomic, Molecular, and Optical Physics* **88**, 063606 (2013).
- [102] M. SPIVAK, *PHYSICS FOR MATHEMATICIANS MECHANICS I* (PUBLISH OR PERISH, INC., 2010).
- [103] D. Witthaut, F. Trimborn, and S. Wimberger, Dissipation-induced coherence and stochastic resonance of an open two-mode bose-einstein condensate, *Physical Review A—Atomic, Molecular, and Optical Physics* **79**, 033621 (2009).
- [104] A. Jacobo, D. Gomila, M. A. Matías, and P. Colet, Effects of noise on excitable dissipative solitons, *The European Physical Journal D* **59**, 37 (2010).